FMSD
(Authors' version)

Finite Controlled Invariants for Sampled Switched Systems

L. Fribourg · U. Kühne · R. Soulat

Abstract We consider in this paper switched systems, a class of hybrid systems recently used with success in various domains such as automotive industry and power electronics. We propose a state-dependent control strategy which makes the trajectories of the analyzed system converge to finite cyclic sequences of points. Our method relies on a technique of *decomposition* of the state space into local regions where the control is uniform. We have implemented the procedure using zonotopes, and applied it successfully to several examples of the literature and industrial case studies in power electronics. [1]

Keywords Hybrid systems, Control synthesis, Limit cycles, Zonotopes, Safety, Controlled invariant

1 Introduction

Sampled switched systems are more and more used in electrical and mechanical industry, e.g. power electronics and automotive industry. This is due to their flexibility and simplicity for controlling accurately industrial mechanisms. These systems are governed by piecewise dynamics that are periodically sampled with a given period τ (see, e.g., [5]). At each sampling time, the "mode" of the system, i.e. the parameters of the dynamics, are switched according to a

L. Fribourg, R. Soulat
LSV, ENS Cachan & CNRS
Cachan, France
E-mail: {fribourg,soulat}@lsv.ens-cachan.fr

U. Kühne
Group of Computer Architecture
University of Bremen, Germany
E-mail: ulrichk@informatik.uni-bremen.de

[1] A short version of this paper appears in *Proc. Reachability Problems 2013, LNCS, vol. 8169, Springer, pages 135-145* under the title "Stability Controllers for Sampled Switched Systems".

control rule. A classical example of sampled switched system is the boost DC-DC converter [3]. The control of a switching cell puts the system, according to its position (open or closed), into one of two modes. When the system stays in the same mode, it evolves towards a unique equilibrium point. In contrast, by adopting switching control rules, one can steer the system to a desired region R that is centered at a different equilibrium point, around which the system oscillates with some variability.

We present here a state-dependent control method which decomposes R into a set of sub-boxes associated with specific control modes: at each sampling time, depending on the location of the system state, one activates a specific mode until the next sampling time. We show that, under certain conditions, the state trajectories converge to a *finite* invariant set of points of R.

1.1 Related work.

Most of the work on computing invariant sets in the context of switched systems has been done for finding the *maximal* controlled invariant set contained in a given region S (see, e.g., [2,5,15]). This approach is very useful when S is known to be a *safe* region, and one wants to find the most permissive controller that allows to stay in this region. Along the lines of the seminal work of Ramadge and Wonham for finite discrete systems [19], the computation of maximal controlled invariant sets is generally done using a *backward* approach, by computing iteratively the intersection of the predecessor sets (or pre-images) of S, until a fixed-point is reached.

Here we use instead an algorithm based on *forward* reachability using a bounded *sequence* of modes (“patterns”), and state-space decomposition.

Similar ideas of exploring bounded mode sequences for controller synthesis for hybrid systems have been recently considered in [6,16,20]. However, all these works use the “indirect” approach in the sense of [2] while we use here the “direct” approach. The direct approach means that the procedure used here works directly on the continuous state space, while in the indirect approach used in [6,16,20], the system is reduced first, via abstraction, to a finite state automaton which bears some bisimilarity property with the original system. An advantage of working directly at the original level is to avoid a potentially costly space discretization operation.

1.2 Plan of the paper

The basic notions of switched systems are presented in Section 2. The basic decomposition procedure for testing controlled invariance is given in Section 3.1; an enhancement of the procedure for ensuring safety is given in Section 3.2. In Section 4, we give theoretical results on the existence of limit cycles, and explain how to compute finite controlled invariants. In Section 5, we illustrate the application of the decomposition procedure to several case studies. We conclude in Section 6.

2 Sampled Switched Affine Systems

Sampled switched *affine* systems, as defined, e.g., in [10], is a subclass of affine hybrid systems [11]. A sampled switched affine system Σ is defined by a triple $\langle \tau, U, \mathcal{F} \rangle$ where:

- $\tau \in \mathbb{R}_{>0}$ is the *time sampling parameter*,
- $U = \{1, \ldots, q\}$ is the finite set of *modes*,
- $\mathcal{F}$ is a set of the form $\{(A_u, B_u)\}_{u \in U}$ with $(A_u, B_u) \in \mathbb{R}^{n \times n} \times \mathbb{R}^{n \times 1}$.

We say that a piecewise $\mathcal{C}^1$ function $\mathbf{x} : \mathbb{R}_{\geq 0} \to \mathbb{R}^n$ is a *trajectory* of Σ if it is continuous and satisfies, for all $k \in \mathbb{N}$:

$$\exists u \in U \ \forall t \in [k\tau, (k+1)\tau) \qquad \dot{\mathbf{x}}(t) = A_u \mathbf{x}(t) + B_u,$$

with $(A_u, B_u) \in \mathcal{F}$. Given $x(0)$, the trajectory is fully determined by the values $u_1, u_2, \ldots$ of u at sampling times $\tau, 2\tau, \ldots$. These values define a control function $\mathbf{u}(t)$, which is constant on each interval $[k\tau, (k+1)\tau)$, for all $k \in \mathbb{N}$. Between two sampling times, the system is governed by a differential equation of the form: $\dot{\mathbf{x}}(t) = A_u \mathbf{x}(t) + B_u$ with $u \in U$ and $(A_u, B_u) \in \mathbb{R}^{n \times n} \times \mathbb{R}^{n \times 1}$. We will use $\mathbf{x}(t, x, u)$ to denote the point reached by Σ at time t under mode u from the initial condition x. This gives a transition relation $\to_u^\tau$ defined by:

$$x \to_u^\tau x' \text{ iff } \mathbf{x}(\tau, x, u) = x' \text{ for } x \text{ and } x' \text{ in } \mathbb{R}^n$$

We define: $\quad Post_u(X) = \{x' \mid x \to_u^\tau x' \text{ for some } x \in X\}$.

Proposition 1 *The mapping* $Post_u : 2^{\mathbb{R}^n} \to 2^{\mathbb{R}^n}$ *with* $u \in U$ *is an affine transformation. The image of a (compact) convex set* X *by* $Post_u$ *with* $u \in U$ *is therefore a (compact) convex set.*

Proof Given a mode $u \in U$, we have that $\dot{\mathbf{x}}(t) = A_u \mathbf{x}(t) + B_u$ with $u \in U$ and $(A_u, B_u) \in \mathbb{R}^{n \times n} \times \mathbb{R}^{n \times 1}$. Therefore, we have that $\mathbf{x}(\tau, x, u) = C_u \cdot x + D_u$ with $C_u = e^{A_u \tau}$ and $D_u = (e^{A_u \tau} - \mathcal{I}_n) A_u^{-1} \cdot B_u$ where $\mathcal{I}_n$ denotes the identity matrix (this only holds if A_u is invertible, but in there exists a similar expression if A_u is not invertible). Hence, $Post_u$ is an affine transformation. Therefore, the image of a (compact) convex set X by $Post_u$ with $u \in U$ is a (compact) convex set. □

Definition 1 (Contractive mode) We say that a mode $u \in U$ is *contractive* if there exists $0 < \beta_u < 1$ such that, for all $x, y \in \mathbb{R}^n$: $\|\mathbf{x}(\tau, x, u) - \mathbf{x}(\tau, y, u)\| \leq \beta_u \|x - y\|$, for some norm $\| \cdot \|$ on $\mathbb{R}^n$. This is equivalent to say $|||e^{A_u \tau}||| = \beta_u$ (i.e., $\sup_{x \neq 0} \frac{\|e^{A_u \tau} x\|}{\|x\|} = \beta_u$) for some $0 < \beta_u < 1$.

Remark 1 The contractivity property of mode u implies that A_u has eigenvalues with negative real parts (A_u is Hurwitz) and that the system associated to mode u is stable. Conversely, if A_u is Hurwitz, then there exists $\tau_{min} > 0$ such that, for all $t > \tau_{min}$, $\|\mathbf{x}(t, x, u) - \mathbf{x}(t, y, u)\| \leq \beta_u \|x - y\|$ for some $0 < \beta_u < 1$. In Definition 1, we thus implicitly require that $\tau > \tau_{min}$.

Definition 2 (Invariance) Given a set $R \subset \mathbb{R}^n$, we say that a zone X is *R-invariant via mode u* if: $Post_u(X) \subseteq R$.
We say that X is *controlled invariant* if: $\forall x \in X\ \exists u \in U\ \exists x' \in X\ x \to_u^\tau x'$.

We will group modes together into sequences called “patterns”. A *k-pattern* is a pattern (sequence of modes) of length at most k. Given a pattern π of the form $(u_1 \cdots u_m)$, let $Post_\pi(X) = \{x' \mid x \to_{u_1}^\tau \cdots \to_{u_m}^\tau x' \text{ for some } x \in X\}$. The notions of R-invariance and contraction extend naturally to patterns. Given a set $R \subset \mathbb{R}^n$, we say that a set X is *R-invariant via* π if $Post_\pi(X) \subseteq R$. Likewise, we say that a pattern $\pi \in U^*$ is *contractive* if

$$\forall x, y \in \mathbb{R}^n \|Post_\pi(x) - Post_\pi(y)\| < \|x - y\|$$

for some norm $\|\cdot\|$ of $\mathbb{R}^n$.

From Proposition 1, it follows:

Proposition 2 *Let π be a pattern. Then the mapping $Post_\pi : 2^{\mathbb{R}^n} \to 2^{\mathbb{R}^n}$ is an affine transformation. The image of a (compact) convex set X by $Post_\pi$ is therefore a (compact) convex set.*

Example 1 (**Boost DC-DC converter**) This example is taken from [3] (see also, e.g., [4,10,21]). This is a boost DC-DC converter with one switching cell (see Figure 1). There are two operation modes depending on the position of the switching cell. An example of pattern of length 4 is illustrated on Figure 2: it corresponds to the application of mode 2 on $(0, \tau]$ and mode 1 on $(\tau, 4\tau]$. The controlled system is steered to a zone where the output voltage stabilizes around a desired value. The range of variations of the output voltage and inductor current is limited in order to avoid phenomena of inductor saturation and blocking voltage stress of the switch. This is defined by a safety area. The state of the system is $x(t) = [i_l(t), v_c(t)]^T$ where i_l is the current intensity in the inductor, and $v_c(t)$ the voltage of the capacitor. The dynamics associated with mode u is of the form $\dot{x}(t) = A_u x(t) + B_u$ $(u = 1, 2)$ with

$$A_1 = \begin{pmatrix} -\frac{r_l}{x_l} & 0 \\ 0 & -\frac{1}{x_c}\frac{1}{r_0+r_c} \end{pmatrix} \quad B_1 = \begin{pmatrix} \frac{v_s}{x_l} \\ 0 \end{pmatrix}$$

$$A_2 = \begin{pmatrix} -\frac{1}{x_l}(r_l + \frac{r_0.r_c}{r_0+r_c}) & -\frac{1}{x_l}\frac{r_0}{r_0+r_c} \\ \frac{1}{x_c}\frac{r_0}{r_0+r_c} & -\frac{1}{x_c}\frac{r_0}{r_0+r_c} \end{pmatrix} \quad B_2 = \begin{pmatrix} \frac{v_s}{x_l} \\ 0 \end{pmatrix}$$

We will use the numerical values of [3], expressed in the per unit system: $x_c = 70$, $x_l = 3$, $r_c = 0.005$, $r_l = 0.05$, $r_0 = 1$, $v_s = 1$. The sampling period is $\tau = 0.5$.

Definition 3 Given a set $R \subseteq \mathbb{R}^n$ and a set $\{(V_i, \pi_i)\}_{i \in I}$ where I is a finite set of indices, V_i is a subset of $\mathbb{R}^n$ (for all $i \in I$), π_i is a k-pattern (for all $i \in I$), we say that $\Delta = \{(V_i, \pi_i)\}_{i \in I}$ is a *k-invariant decomposition of* R if:

- $R = \bigcup_{i \in I} V_i$, and
- V_i is R-invariant via π_i (i.e., $Post_{\pi_i}(V_i) \subseteq R$), for all $i \in I$.

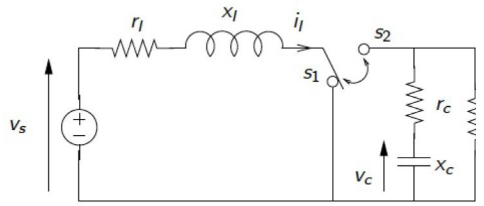

Fig. 1: Scheme of the boost DC-DC converter

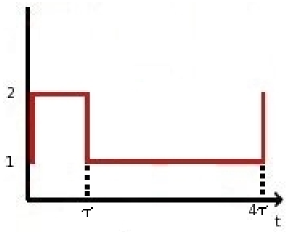

Fig. 2: Cell switching for pattern $(2 \cdot 1 \cdot 1 \cdot 1)$

In the following, the set R will be referred to as a *global (control) box*, and the V_is $(i \in I)$ as *local (control) boxes*.

Given a set $R \subseteq \mathbb{R}^n$ and a set Δ of the form $\{(V_i, \pi_i)\}_{i \in I}$ with $\bigcup_{i \in I} V_i = R$, we define $Post_\Delta$ as follows:

$$Post_\Delta(X) = \bigcup_{i \in I} Post_{\pi_i}(X \cap V_i), \quad \text{for all } X \subseteq R.$$

We have:

Proposition 3 *Given a set $R \subseteq \mathbb{R}^n$ and a set $\Delta : \{(V_i, \pi_i)\}_{i \in I}$ with $\bigcup_{i \in I} V_i = R$, we have:*

- *Δ is a k-invariant decomposition of R iff $Post_\Delta(R) \subseteq R$.*
- *The image of a (compact) convex set X by $Post_\Delta$ is a finite union of (compact) convex sets.*

NB: For the sake of simplicity, we will use $Post_\Delta(x)$ instead of $Post_\Delta(\{x\})$, when x is a point of $\mathbb{R}^n$.

Example 2 In the case of the Boost DC-DC converter, one can show that, for $R = [1.55, 2.15] \times [1.0, 1.4]$, there is a decomposition $\Delta = \{(V_i, \pi_i)\}_{i=1,\ldots,4}$ with $V_1 = [1.55, 1.85] \times [1.0, 1.2]$, $V_2 = [1.85, 2.15] \times [1.0, 1.2]$, $V_3 = [1.85, 2.15] \times [1.2, 1.4]$, $V_4 = [1.55, 1.85] \times [1.2, 1.4]$, and $\pi_1 = (1 \cdot 1 \cdot 2 \cdot 2 \cdot 2)$, $\pi_2 = (2)$, $\pi_3 = (2 \cdot 1 \cdot 2)$, $\pi_4 = (1)$. One can check indeed that, for all $1 \leq i \leq 4$, $Post_{\pi_i}(V_i) \subseteq R$. This is visualized on Figure 3. In Section 3, we will explain how to generate such a decomposition.

Definition 4 Given a pattern π of the form $(u_1 \cdots u_m)$, and a set X, the *unfolding of X via π*, denoted by $Unf_\pi(X)$, is the set $\bigcup_{i=0}^{m} X_i$ with:

- $X_0 = X$,
- $X_{i+1} = Post_{u_{i+1}}(X_i)$, for all $0 \leq i \leq m-1$.

NB: Note that we have $X_m = Post_\pi(X)$.

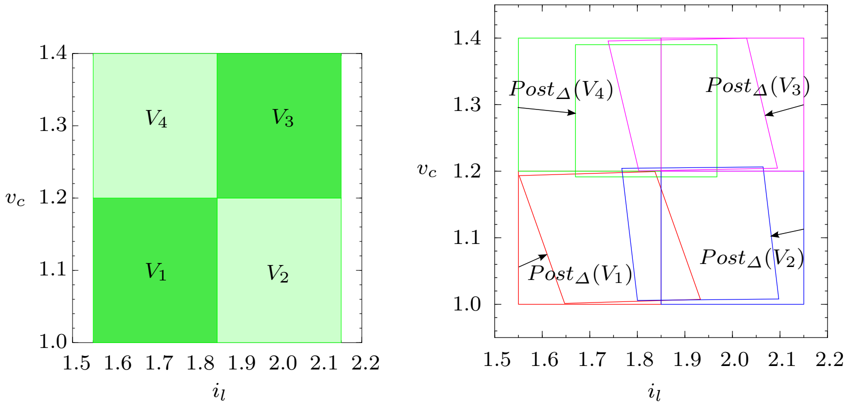

Fig. 3: Decomposition Δ of R for the Boost DC-DC converter example (left), and visualization of $Post_\Delta(R) \subseteq R$ (right)

Definition 5 Consider a k-invariant set R of decomposition $\Delta = \{(V_i, \pi_i)\}_{i \in I}$. The Δ-*unfolding* of R, denoted by $Unf_\Delta(R)$, is the set:

$$\bigcup_{i \in I} Unf_{\pi_i}(V_i).$$

Example 3 Figure 4 depicts the unfolding of R for the decomposition Δ of example 2, where light red (resp. dark blue) indicates that mode 1 (resp. 2) applies.

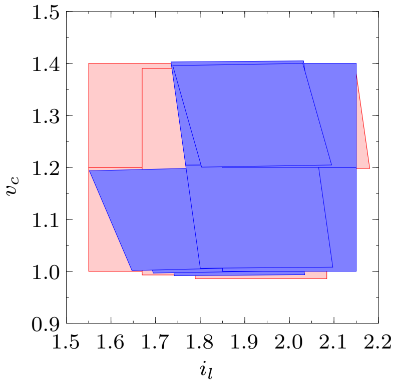

Fig. 4: Δ-unfolding of $R = [1.55, 2.15] \times [1.0, 1.4]$ in the Boost DC-DC converter example where light red (resp. dark blue) zones indicate that mode 1 (resp. 2) applies

Proposition 4 *Suppose that a set R has a k-invariant decomposition Δ. Then the Δ-unfolding of R is controlled invariant.*

Proof Let us explain how such a control can be refined in order to make R', the Δ-unfolding of R, *controlled invariant.* We extend $\Delta : \{(V_i, \pi_i)\}_{i\in I}$ each element (V_i, π_i) where π_i is of the form $(u_i^1 u_i^2 \cdots u_i^m)$, by m couples of the form (V_i^1, u_i^1), (V_i^2, u_i^2), $\ldots$, (V_i^m, u_i^m) with $V_i^1 = V_i$, $V_i^2 = Post_{u_i^1}(V_i^1)$,$\ldots$, $V_i^m = Post_{u_i^{m-1}}(V_i^{m-1})$. This yields an extended decomposition Δ' of the form $\{(W_i, u_i)\}_{i\in I'}$ with $\bigcup_{i\in I'} W_i = R'$ and $Post_{u_i}(W_i) \subseteq R'$ for all $i \in I'$. Hence, for each $x \in R'$, x belongs to W_i for some $i \in I'$, and $Post_{u_i}(x) \subseteq R'$. This shows that R' is controlled invariant. □

2.1 Control induced by the decomposition

The decomposition Δ induces a state-dependent control that makes any trajectory starting from R go back to R within at most k steps: Given a starting state x_0 in R, we know that $x_0 \in V_i$ for some $i \in I$ (since $R = \bigcup_{i\in I} V_i$); one thus applies π_i to x_0, which gives a new state x_1 that belongs to R (since V_i is R-invariant via π_i); the process is repeated on x_1, and so on iteratively. Given a point $x \in R$, we will denote by $succ_\Delta(x)$ the point of R obtained by applying π_i to x when x is in V_i. Note that a nondeterministic choice has to be done when a point x belongs to more than one local box V_i. We will suppose that we have an implicit selection function that operates a nondeterministic choice in such a case (for example, one can select the set V_i of least index containing x). When x belongs to a single local box V_i, then $succ_\Delta(x) = Post_\Delta(x)$.

A sequence of points $\{x_i\}_{i\geq 0}$ (with $x_{i+1} = succ_\Delta(x_i)$ for all $i \geq 0$) will be called a *discrete trajectory induced by Δ*, or more simply, a *Δ-trajectory.* [2]

We will also consider the *unfolding* of a Δ-trajectory, which corresponds to considering not only the successors of points via patterns, but also all the intermediate points generated by intermediate application of the modes forming the patterns. In the figures, for the sake of clarity, the points of Δ-trajectories will be linked together using straight lines, and similarly for their unfoldings.

A Δ-trajectory starting from the left upper corner of $R = [1.55, 2.15] \times [1.0, 1.4]$ for the Boost example, is presented in Figure 5 together with its unfolding.

Using Proposition 4, one can prove safety properties of the controlled system, by showing $Unf_\Delta(R) \subseteq S$, where S is known to be a set of safe positions (see Section 3.2).

[2] We will sometimes denote such a trajectory under the form: $x_0 \rightarrow_{\pi_{i_1}} x_1 \rightarrow_{\pi_{i_2}} \cdots$ with $i_1, i_2, \cdots \in I$.

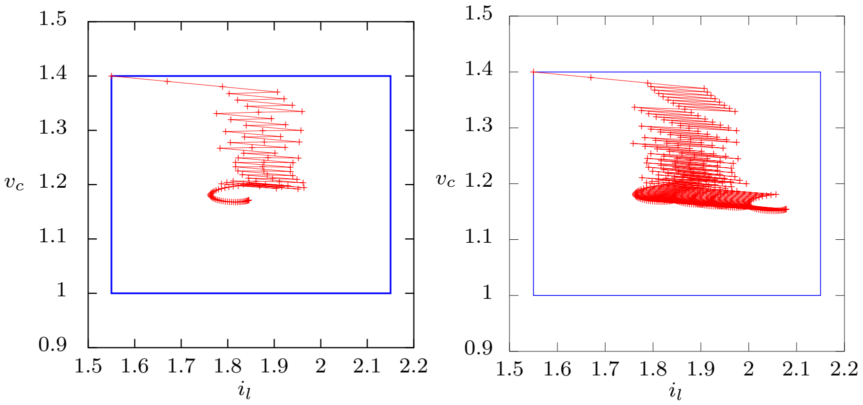

Fig. 5: Δ-trajectory for the Boost example (left), and its unfolding (right)

3 Decomposition Procedure

3.1 Basic procedure

We suppose that we are given a global box $R \subseteq \mathbb{R}^n$. We now give a Decomposition procedure which generates a k-invariant decomposition of R, as follows:

It first calls sub-procedure Find_Pattern in order to get a k-pattern such that R is R-invariant. If it succeeds, then it is done. Otherwise, it divides R into 2^n sub-boxes $V_1, \dots, V_{2^n}$ of equal size. If for each V_i, Find_Pattern returns a k-pattern making it R-invariant, it is done. If, for some V_j, no such pattern exists, the procedure is recursively applied to V_j. It ends with success when a k-invariant decomposition of R is found, or failure when the maximal degree d of decomposition is reached.

The algorithmic form of the procedure is given in Algorithms 1 and 2. (For the sake of simplicity, we consider the case of dimension $n = 2$, but the extension to higher dimensions $n > 2$ is straightforward.) The main procedure Decomposition(W,R,D,K) is called with R as input value for W, d for input value for D, and k as input value for K; it returns either $\langle \{(V_i, \pi_i)\}_i, True\rangle$ with $\bigcup_i V_i = W$ and $\bigcup_i Post_{\pi_i}(V_i) \subseteq R$, or $\langle \_, False\rangle$. The sub-procedure Find_Pattern(W,R,K) looks for a K-pattern for which W is R-invariant: it selects all the K-patterns (which are in finite number) by non-decreasing length order until either it finds such a pattern π (output: $\langle \pi, True\rangle$), or none exists (output: $\langle \_, False\rangle$).

The correctness of the procedure is stated as follows.

Theorem 1 *If Decomposition(R,R,d,k) returns $\langle \Delta, True\rangle$, then Δ is a k-invariant decomposition of R. (Hence, $Unf_\Delta(R)$ is controlled invariant.)*

Remark 2 Since we consider closed boxes, two adjacent boxes V_i and V_j share a common facet.

Remark 3 In case the procedure Decomposition(R,R,d,k) does not succeed to find a valid decomposition with depth d and length k, a partial result can still be obtained. For this purpose, it is checked in an additional step, if those regions $R' \subset R$ for which a pattern could be found constitute an invariant set, i.e. if $Post_{\Delta}(R') \subseteq R'$.

A sufficient condition for the existence of a decomposition is given in Appendix 1.

Algorithm 1: Decomposition(W,R,D,K)

```
Input: A box $W$, a box $R$, a degree $D$ of decomposition, a length $K$ of pattern
Output: $\langle \{(V_i, \pi_i)\}_i, True \rangle$ with $\bigcup_i V_i = W$ and $\bigcup_i Post_{\pi_i}(V_i) \subseteq R$, or $\langle \_, False \rangle$
$(\pi, b) := Find\_Pattern(W, R, K)$
if $b = True$ then
    return $\langle \{(W, \pi)\}, True \rangle$
else
    if $D = 0$ then
        return $\langle \_, False \rangle$
    else
        Divide equally $W$ into $(W_1, W_2, W_3, W_4)$    /* (case $n = 2$)    */
        $(\Delta_1, b_1)$ := Decomposition($W_1$,$R$,$D-1$,$K$)
        $(\Delta_2, b_2)$ := Decomposition($W_2$,$R$,$D-1$,$K$)
        $(\Delta_3, b_3)$ := Decomposition($W_3$,$R$,$D-1$,$K$)
        $(\Delta_4, b_4)$ := Decomposition($W_4$,$R$,$D-1$,$K$)
        return $(\Delta_1 \cup \Delta_2 \cup \Delta_3 \cup \Delta_4, b_1 \wedge b_2 \wedge b_3 \wedge b_4)$
```

Algorithm 2: Find_Pattern(W,R,K)

```
Input: A box $W$, a box $R$, a length $K$ of pattern
Output: $\langle \pi, True \rangle$ with $Post_{\pi}(W) \subseteq R$, or $\langle \_, False \rangle$ when no pattern maps $W$ into
        $R$
for $i = 1 \dots K$ do
    $\Pi$ := set of patterns of length $i$
    while $\Pi$ is non empty do
        Select $\pi$ in $\Pi$
        $\Pi := \Pi \setminus \{\pi\}$
        if $Post_{\pi}(W) \subseteq R$ then
            return $\langle \pi, True \rangle$
return $\langle \_, False \rangle$
```

3.2 Enhancement for safety

Let us now explain how to extend the decomposition procedure in order to show additionally that we have $Unf_{\Delta}(R) \subseteq S$, where S is a given safety set containing R. This is done by adding an extra-input argument to procedures Decomposition and Find_Pattern corresponding to S. We then replace line 1 of Decomposition(W,R,D,K,S) by Find_Pattern(W,R,K,S), and line 6 of procedure Find_Pattern by:

If $Post_\pi(W) \subseteq R$ ***And*** $Unf_\pi(W) \subseteq S$ **then**

In other words: if π is a pattern of the form $(u_1 \cdots u_m)$ with $u_1, ..., u_m \in U$, we check additionally $W_i \subseteq S$ for all $1 \leq i \leq m$, where the W_i's are the intermediate sets defined by $W_1 = Post_{u_1}(W)$, ..., $W_m = Post_{u_m}(W_{m-1})$ We have:

Theorem 2 *If the procedure Decomposition(R,R,d,k,S) returns* $\langle \Delta, True \rangle$, *then* $Unf_\Delta(R)$ *is controlled invariant. Furthermore, we have:* $Unf_\Delta(R) \subseteq S$.

Hence, the system under the control inferred by the procedure (when it succeeds), is guaranteed to be safe. The procedure has been implemented in Octave [1] using zonotopes [13] in order to represent and manipulate efficiently boxes and convex polytopes. They allow us to extend easily the decomposition procedure in order to allow for small perturbations of the system dynamics (see Appendix 3 for details).

4 Finite Controlled Invariants and Limit cycles

4.1 Theoretical results

We suppose that we are given a global box R and a decomposition $\Delta = \{(V_i, \pi_i)\}_{i \in I}$ produced by the decomposition algorithm of Section 3. We denote the union of the set of borders of V_i ($i \in I$) by $\partial\Delta$. (Recall that two adjacent boxes V_i and V_j share a common border; see Remark 2.)

We show how to produce *finite* controlled invariant sets using the iteration of $Post_\Delta$ on R. The idea is like this: Since $Post_\Delta(R) \subseteq R$, one has $Post_\Delta^{i+1}(R) \subseteq Post_\Delta^{i}(R)$ for all $i \geq 0$, and the limit set $R_\Delta^\infty = \bigcap_{i \geq 0} Post_\Delta^i(R)$ is well defined and non-empty. We will show that under certain assumptions, R_Δ^∞ is *finite* and made of disjoint subsets, which correspond to "limit cycles": each limit cycle is a set of points of $\mathbb{R}^n$ of the form $\{y_0, y_1, \ldots, y_{m-1}\}$ with $y_0 \rightarrow_{\pi_{i_1}} y_1 \rightarrow_{\pi_{i_2}} \cdots \rightarrow_{\pi_{i_m}} y_m = y_0$. Each Δ-trajectory starting from a point of R converges to a limit cycle of R_Δ^∞. Furthermore, the Δ-unfolding of each limit cycle is a controlled invariant set. We make the following assumptions:

(H1): All the modes are contractive in R for a common norm $\| \cdot \|$ on $\mathbb{R}^n$.
(H2): There exists $N \in \mathbb{N}$ such that $Post_\Delta^N(R) \cap \partial\Delta = \emptyset$.

As seen in Remark 1, assumption (H1) implies that all the matrices A_u ($u \in U$) are Hurwitz and stable. A sufficient condition for (H1) is the existence of a quadratic common Lyapunov function for all matrices A_u, the norm being then associated to the Lyapunov function and not the usual Euclidean norm (see, e.g., [14]). Assumption (H2) is justified as follows. When $Post_\Delta$ is applied to R for the first time, the local boxes are transformed to $|I|$ convex sets. If such a set, say W, crosses a border of $\partial\Delta$ and partly belongs to, say, two local boxes V_1 and V_2, it will be split into two sets $Post_{\pi_1}(W \cap V_1)$ and $Post_{\pi_2}(W \cap V_2)$ at the next application of $Post_\Delta$. The number of convex sets generated at each application of $Post_\Delta$ thus increases repeatedly until no image crosses a border, which happens at step N by assumption (H2). As shown below, the images generated by further application of $Post_\Delta$ will then never cross $\partial\Delta$: these images will either disappear or shrink towards single points by assumption (H1). Let us consider the (compact) convex sets W^k_σ where $k \in \mathbb{N}$ and $\sigma \in I^k$, defined as follows:

- $W^0_\varepsilon = R$ where ε denotes the empty sequence.
- $W^{k+1}_{(i\cdot\sigma)} = Post_{\pi_i}(W^k_\sigma \cap V_i)$ with $i \in I$ and $\sigma \in I^k$.

It is easy to show that, for all $k \in \mathbb{N}$ and all $\sigma \in I^k$, W^k_σ is a compact convex set such that
(1): $Post^k_\Delta(R) = \bigcup_{\sigma \in I^k} W^k_\sigma$.
It follows from assumption $(H2)$ that, for all sequence $\sigma \in I^N$, $W^N_\sigma \cap \partial\Delta = \emptyset$, therefore $W^N_\sigma \subseteq \overset{\circ}{V_i}$ for some $i \in I$, and $Post_\Delta(W^N_\sigma) = Post_{\pi_i}(W^N_\sigma)$. Since $Post^{N+1}_\Delta(R) \subseteq Post^N_\Delta(R)$, $Post_\Delta(W^N_\sigma) = Post_{\pi_i}(W^N_\sigma)$ is a compact convex set included in $Post^N_\Delta(R)$, and is therefore included in one of the convex components of $Post^N_\Delta(R)$. We have
(2): $Post_\Delta(W^N_\sigma) \subseteq W^N_{\sigma'}$ for some $\sigma' \in I^N$.
Now, for all Δ-trajectory $\{x_0, x_1, \dots\}$, we have
(3): $\forall k \geq N \ \exists \sigma \in I^N : \ x_k \in W^N_\sigma$
because, for all $k \geq N$, $x_k \in Post^k_\Delta(R) \subseteq Post^N_\Delta(R) = \bigcup_{\sigma \in I^N} W^N_\sigma$. By rewriting the elements of $\{W^N_\sigma\}_{\sigma \in I^N}$ under the form $\{W_1, \dots, W_M\}$, and denoting the set $\{1, \dots, M\}$ by J, we recapitulate these results as follows:

Proposition 5 *There exist M compact convex sets $W_1, \dots, W_M$ with $\bigcup_{j=1}^M W_j \cap \partial\Delta = \emptyset$, such that*
$(1')$: $Post^N_\Delta(R) = \bigcup_{j=1}^M W_j$
$(2')$: $\forall j \in J \ \exists j' \in J : \ Post_\Delta(W_j) \subseteq W_{j'}$.
$(3')$: for all Δ-trajectory $\{x_0, x_1, \dots\}$, $\forall i \geq N \ \exists j \in J : \ x_i \in W_j$.
The element j' associated with j in $(2')$ will be denoted by $s(j)$. (If there are more than one such a j', an arbitrary one is selected.)

Using part $(2')$ of Proposition 5, one can define a directed graph where J is the set of vertices, and there is an oriented edge from $j \in J$ to $j' \in J$ iff $j' = s(j)$ (i.e., $Post_\Delta(W_j) \subseteq W_{j'}$). The strongly connected components of this graph are cyclic (because each vertex of the graph has a unique outgoing edge).

In the following, we will denote a cyclic subgraph by $\mathcal{C} = (j_0, \dots, j_{m-1})$ with $j_{\ell+1} = s(j_\ell)$ for $0 \leq \ell \leq m-1$, using the convention: $j_m = j_0$. For every element j of $\mathcal{C}$, we have $s^m(j) = j$, i.e.: $Post^m_\Delta(W_j) \subseteq W_j$. More generally, $Post^{(i+1)\cdot m}_\Delta(W_j) \subseteq Post^{i\cdot m}_\Delta(W_j)$. We can define a decreasing sequence of nonempty compact convex sets $Post^{i\cdot m}_\Delta W_j$ for all $i \geq 0$. The limit set $\bigcap_{i\geq 0} Post^{i\cdot m}_\Delta(W_j)$ is a nonempty compact set. Furthermore, since by (H1) all the modes are contractive, it is easy to see than this limit set is reduced to a point, that will be denoted by z_j. Every cycle of indices $\mathcal{C} = (j_0, \dots, j_{m-1})$ thus corresponds to a cycle of points $Z_{\mathcal{C}} = (z_{j_0}, \dots, z_{j_{m-1}})$. Furthermore, it is easy to show that, for all $0 \leq \ell \leq m-1$, we have $succ_{\Delta}(z_{j_\ell}) = z_{j_{\ell+1}}$. Let us denote the set of vertices of all the cyclic subgraphs by J'. An illustration of the form of such a graph is given in Figure 6. We recapitulate the above results as follows:

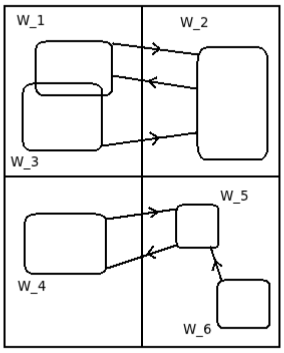

Fig. 6: Illustration of the graph of W_js with $J = \{1, 2, 3, 4, 5, 6\}$ and $J' = \{1, 2, 4, 5\}$

Proposition 6 *For all cycle $\mathcal{C} = (j_0, \dots, j_{m-1})$ of J', we have*
$\forall j \in \mathcal{C}: \quad Post^m_{\Delta}(W_j) \subseteq W_j.$
Furthermore, for all $j \in \mathcal{C}$, the set $\bigcap_{i \geq 0} Post^{i \cdot m}_{\Delta}(W_j)$ is well defined and equal to a point denoted by z_j. We have, for all $\ell = 0, \dots m-1$: $succ_{\Delta}(z_{j_\ell}) = z_{j_{\ell+1}}$.

Consider now the vertices of the graph that are $J \setminus J'$. Each of them is the destination of a finite number of acyclic paths. This means that after a finite number of iterations of $Post_{\Delta}$, no point will belong to W_j for $j \in J \setminus J'$[3]. Formally: $\exists N' \geq N \; \forall j \in J \setminus J' \; Post^{N'}_{\Delta}(R) \cap W_j = \emptyset$. Furthermore: $\forall k \geq N'$ $Post^k_{\Delta}(R) \subseteq \bigcup_{j \in J'} W_j$. It follows that, for all Δ-trajectory $\{x_0, x_1, \dots\}$, $x_{N'}$ belong to W_j for some $j \in J'$. Let $\mathcal{C} = (j_0, \dots, j_{m-1})$ be the cycle which contains j. Modulo a circular permutation of $\mathcal{C}$, one can suppose $j = j_0$. Then, for all $0 \leq \ell \leq m-1$, $x_{N'+\ell}$ belongs to W_{j_ℓ}. More generally, $x_{N'+i \cdot m+\ell} \in Post^{i \cdot m}(W_{j_\ell})$. It follows: $\lim_{i \to \infty} x_{N'+i \cdot m+\ell} = \bigcap_{i \geq 0} Post^{i \cdot m}(W_{j_\ell}) = z_{j_\ell}$. We have:

Theorem 3 *Every Δ-trajectory $\{x_0, x_1, \dots\}$ converges to a limit cycle in the following sense: for each initial point $x_0 \in R$, there exists a cycle $\mathcal{C} = (j_0, \dots, j_{m-1})$ of J', a cycle of points $Z_{\mathcal{C}} = (z_{j_0}, \dots, z_{j_{m-1}})$ and an integer $N' \in \mathbb{N}$ such that, for all $\ell = 0, \dots, m-1$*

[3] More formally, no point will belong to a W_j for $j \in J \setminus J'$ if it does not belong to a $W_{j'}$ for $j' \in J'$.

- $\forall i \geq 0: \; x_{N'+i\cdot m+\ell} \in Post^{i\cdot m}(W_{j_\ell}) \subseteq W_{j_\ell}$.
- $\lim_{i\to\infty} x_{N'+i\cdot m+\ell} = z_{j_\ell}$.
- $Post^{m}_{\Delta}(z_{j_\ell}) = z_{j_\ell}$

The expression $Post^{m}_{\Delta}(z_{j_\ell}) = z_{j_\ell}$ of Theorem 3 gives a practical method to compute z_{j_ℓ} ($\ell = 0, \ldots, m-1$). Indeed, we have that $z_{j_\ell} \in V_i$ for some $i \in I$. Let us denote such a i by $\phi(j_\ell)$, and let $\pi = (\pi_{\phi(j_0)} \cdots \pi_{\phi(j_{m-1})})$. Since $Post^{m}_{\Delta}(z_{j_0}) = Post_{\pi}(z_{j_0}) = C_\pi \cdot z_{j_0} + D_\pi$ for some matrix C_π and vector D_π, we can compute z_{j_0} as a solution of the equation $z_{j_0} = C_\pi \cdot z_{j_0} + D_\pi$. Similar equations hold for z_{j_ℓ} with $\ell = 1, \ldots, m-1$. Furthermore, we have:

Proposition 7 $R^{\infty}_{\Delta} = \{z_j \mid j \in J'\}$.

Proof We know that there exists $K > 0$ such that, for all $k \geq K$, $Post^{k}_{\Delta}(R) = \bigcup_{j\in J'} Post^{k}_{\Delta}(W_j)$. We also know: $\bigcap_{k\geq 0} Post^{k}_{\Delta}(W_j) = \{z_j\}$. It follows $R^{\infty}_{\Delta} = \bigcap_{k\geq 0} Post^{k}_{\Delta}(R) = \bigcup_{j\in J'} \bigcap_{k\geq 0} Post^{k}_{\Delta}(W_j) = \{z_j \mid j \in J'\}$. □

The elements of $\{z_j \mid j \in J'\}$ are grouped together into cyclic sets of points. For all cyclic set of points $Z_{\mathcal{C}}$, we have $Post_{\Delta}(Z_{\mathcal{C}}) = Z_{\mathcal{C}}$. It follows:

Proposition 8 *For all cyclic set of points $Z_{\mathcal{C}}$, the Δ-unfolding of $Z_{\mathcal{C}}$ is a controlled invariant set.*

Note that, although the Δ-unfolding of $Z_{\mathcal{C}}$ is finite, it is not necessarily *minimal*. There may indeed exist a *strict* subset of the Δ-unfolding of $Z_{\mathcal{C}}$ of the form, say $\{y_0, \ldots, y_{p-1}\}$, that is itself controlled invariant, i.e., such that: $y_0 \to_{u_1} y_1 \to_{u_2} \cdots \to_{u_p} y_p = y_0$ for some $u_1, \ldots, u_p \in U$.

4.2 Discussion of the assumptions (H1) and (H2)

Under assumptions (H1) and (H2), we have shown that the trajectories converge to a finite cyclic set of points. Assumption (H1) of contractivity of the modes can be relaxed by considering the patterns of the decomposition instead of the modes. In practice, we may observe the convergence to finite cyclic sets of points even in the absence of contractivity, such as in the helicopter motion example (see Figure 18).

In the absence of assumption (H2), the number of connected sets of $Post^{k}_{\Delta}(R)$ can increase indefinitely. Assumption (H2) thus seems to be a necessary condition for the finiteness of R^{∞}_{Δ}. An exception could correspond to the case where a point of a limit cycle belongs to a border of the decomposition Δ.

In Appendix 4, we give an example where the modes of the Δ-decomposition are not contractive, and for which R^{∞}_{Δ} is infinite.

4.3 Illustrative examples

Boost DC-DC Converter We consider box $R = [1.55, 2.15] \times [1.0, 1.4]$. One can check that all the modes of the Boost DC-DC converter are contractive.

One can also see that in the Boost DC-DC Converter, there exists $N \in \mathbb{N}$ such that $Post_{\Delta}^{N}(R)$ is strictly included in V_1 (See Appendix 5). Therefore, in such a case, the limit cycle is reduced to a unique point $y_0 \in V_1$. We have: $y_0 \to_{\pi_1} y_1 = y_0$, with $\pi_1 = (1 \cdot 1 \cdot 2 \cdot 2 \cdot 2)$:

The unfolding of this limit cycle is depicted in Figure 7.

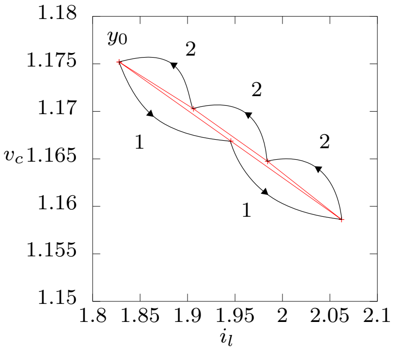

Fig. 7: Δ-unfolding of the limit cycle $\{y_0\}$ for the Boost example

Two tanks The two-tank system example is taken from [12]. The system consist of two tanks and two valves. The first valve adds to the inflow of tank 1, the second valve is a drain valve for tank 2. There is also a constant outflow from tank 2 caused by a pump. The system is linearized at a desired operating point. The objective is to keep the water level in both tanks within limits using a discrete open/close switching strategy for the valves. Let the water level of tank 1 and 2 be given by x_1 and x_2 respectively. The behavior of x_1 is given by: $\dot{x}_1 = -x_1 - 2$ when the tank 1 valve is closed, and $\dot{x}_1 = -x_1 + 3$ when it is closed. Likewise, x_2 is driven by: $\dot{x}_2 = x_1$ when the tank 2 valve is closed and $\dot{x}_2 = x_1 - x_2 - 5$ when it is closed.

Using $R = [-1.5, 2.5] \times [-0.5, 1.5]$ as a control box, we obtain the decomposition depicted in Figure 8. With $V_1 = [-1.5, 0.5] \times [-0.5, 0.5]$ associated to pattern $\pi_1 = (2 \cdot 3 \cdot 3)$, $V_2 = [0.5, 2.5] \times [-0.5, 0.5]$ to $\pi_2 = (2)$, $V_3 = [0.5, 2.5] \times [0.5, 1.5]$ to $\pi_3 = (1 \cdot 4)$ and $V_4 = [-1.5, 0.5] \times [0.5, 1.5]$ to $\pi_4 = 3$.

One can check that all the modes of the two-tank system are contractive. One can also check that there exists $N \in \mathbb{N}$ such that $Post_{\Delta}^{N}(R)$ does not intersect the borders of Δ.

Figure 9 depicts a discrete trajectory of the two tank system, and its Δ-unfolding.

The limit cycle is of the form $\{y_0, y_1, y_2, y_3\}$ with $y_0 \to_{\pi_2} y_1 \to_{\pi_2} y_2 \to_{\pi_1} y_3 \to_{\pi_3} y_4 = y_0$ (with $\pi_2 = (1)$, $\pi_1 = (2 \cdot 3 \cdot 3)$, $\pi_3 = (1 \cdot 4)$). This limit cycle is depicted on the left of Figure 10, and its Δ-unfolding (corresponding to the sequence $(1 \cdot 1 \cdot 2 \cdot 3 \cdot 3 \cdot 1 \cdot 4)$) on the right.

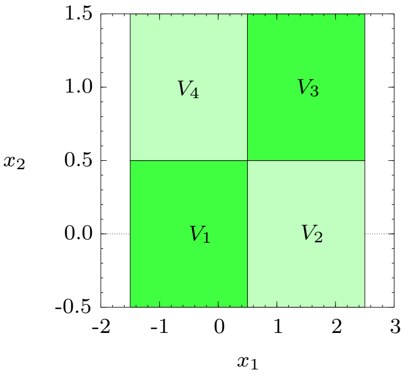

Fig. 8: Decomposition for the two tanks problem

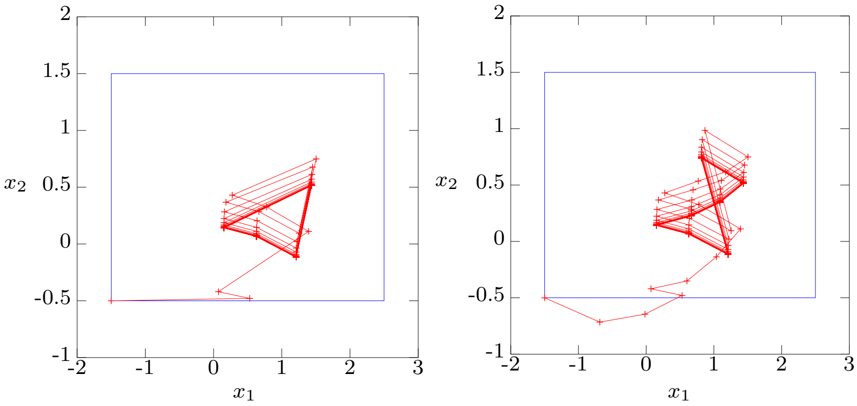

Fig. 9: Δ-trajectory starting from the bottom left corner of R (left), and its Δ-unfolding (right)

5 Implementation and case studies

The implementation of the method is made of two basic procedures: a procedure Decomposition, which outputs Δ, and a procedure, called Iteration which constructs R^i_Δ for $i \geq 0$. The Decomposition procedure makes use of zonotopes [13], and has been written in Octave [1]. The procedure Iteration does not use the data structure zonotopes because it involves the intersection operator which does not preserve the structure of zonotopes. It has been written in Ocaml [17], using the *Parma Polyhedra Library* (PPL [18]). The Iteration procedure receives Δ from module Decomposition and outputs the successive iterations of $Post_\Delta$. The sequence of post sets can also be visualized

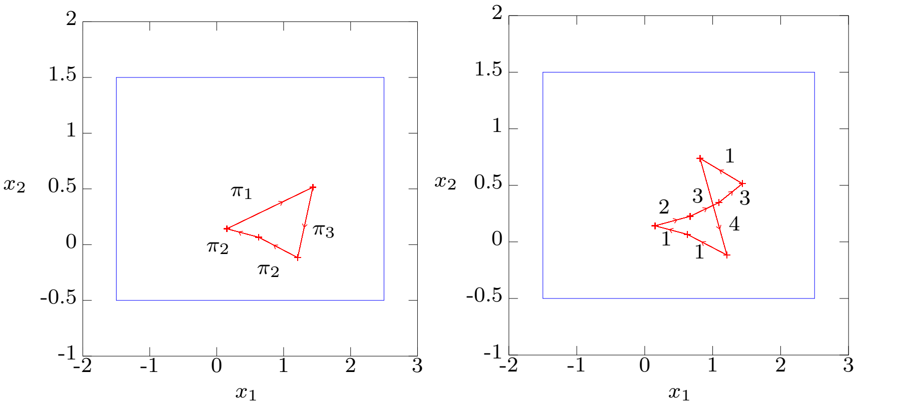

Fig. 10: Limit cycle for the two tanks example (left), and its Δ-unfolding (right)

Table 1: Experimental results

Example	Run-time	#patterns	$\|U\|$	k	d	n	(H1)	(H2)	Cycle
Boost [3]	54 s	12,113	2	10	4	2	yes	yes	yes
Two-tank [12]	4 s	1,423	4	3	1	2	yes	yes	yes
Heating [9]	1 s	134	2	2	4	2	yes	yes	yes
Helicopter [7]	$\approx 2\ h$	$\approx 1.5 \cdot 10^6$	9	6	4	2	no	yes	yes
5-level [8]	60 s	1,688	16	8	1	3	no	yes	yes
7-level [8]	98 min	154,991	64	32	1	5	no	yes	yes

as an animation (see Figure 28 and 29 in Appendix 5). The code is available online[4].

Details on case studies are given in Appendix 2. We give the benchmarks corresponding to the Boost DC-DC Converter, the two-room building heating, the two-tank system the helicopter motion and several case studies on a multilevel converter. All the experiments have been run on a machine equipped with an Intel Core2 CPU X6800 at 2.93GHz and with 2GiB of main memory. The results are shown in Table 1.

The first column indicates the name of the example together with its reference. The second column indicates the running time to obtain a decomposition, and the third one the number of simulated patterns needed to obtain this decomposition[5]. The subsequent columns labeled by $|U|$, k, d and n indicate the number of modes, the input parameter of maximal pattern length, the input parameter of decomposition depth and the space dimension respectively. Fi-

[4] `https://bitbucket.org/ukuehne/minimator`

[5] Note that the number of simulated patterns in the table can be larger than the number of possible patterns for given n and k, since many patterns will be simulated multiple times for different tiles.

nally, the column '(H1)' (resp. '(H2)') indicates if (H1) (resp. (H2)) is satisfied, and the column 'cycle' if the controlled trajectories converge to a limit cycle.

We can see that on the helicopter example, and the 5 and 7-level examples that condition (H1) is not necessary in order to obtain limit cycles.

6 Conclusion

We have presented an original technique to derive attractive limit cycles for controlled trajectories starting in a given region R in the context of sampled switched systems. The control is state-dependent and is induced by a decomposition procedure that returns a set of pairs (subregion, pattern) such that applying a pattern to its related subregion leads to a configuration within R. We have implemented the procedure using zonotopes, and applied it successfully to several examples of the literature and industrial case studies in power electronics (see [8]).

Acknowledgement. We are grateful to the anonymous referees for their numerous helpful remarks.

References

1. Octave Web page. http://www.gnu.org/software/octave/.
2. E. Asarin, O. Bournez, T. Dang, O. Maler, and A. Pnueli. Effective Synthesis of Switching Controllers for Linear Systems. *Proceedings of the IEEE, Special Issue on Hybrid Systems*, 88(7):1011–1025, 2000.
3. A. Beccuti, G. Papafotiou, and M. Morari. Optimal control of the boost dc-dc converter. In *Proc. 44th IEEE Conference on Decision and Control European Control Conference (CDC-ECC '05)*, pages 4457 – 4462, dec. 2005.
4. J. Buisson, P.-Y. Richard, and H. Cormerais. On the stabilisation of switching electrical power converters. In *HSCC*, volume 3414 of *LNCS*, pages 184–197. 2005.
5. J. Cámara, A. Girard, and G. Gößler. Safety controller synthesis for switched systems using multi-scale symbolic models. In *Proc. 50th IEEE Conference on Decision and Control (CDC-ECC '11)*, pages 520–525, 2011.
6. E. L. Corronc, A. Girard, and G. Goessler. Mode sequences as symbolic states in abstractions of incrementally stable switched systems. In *CDC*, pages 3225–3230. IEEE, 2013.
7. J. Ding, E. Li, H. Huang, and C. J. Tomlin. Reachability-based synthesis of feedback policies for motion planning under bounded disturbances. In *IEEE International Conference on Robotics and Automation (ICRA'11)*, pages 2160–2165, 2011.
8. G. Feld, L. Fribourg, D. Labrousse, B. Revol, and R. Soulat. Correct by design control of 5-level and 7-level converters. Research Report LSV-12-25, LSV, ENS Cachan, France, Dec 2012.
9. A. Girard. Low-complexity switching controllers for safety using symbolic models. In M. Heemels, B. De Schutter, and M. Lazar, editors, *4th IFAC conference on Analysis and Design of Hybrid Systems, June, 2012*, Eindhoven, Pays-Bas, 2012.
10. A. Girard, G. Pola, and P. Tabuada. Approximately bisimilar symbolic models for incrementally stable switched systems. *IEEE Trans. on Automatic Control*, 55:116–126, 2010.
11. T. A. Henzinger. The theory of hybrid automata. In *Proceedings of the 11th Annual IEEE Symposium on Logic in Computer Science*, LICS '96, pages 278–292, Washington, DC, USA, 1996. IEEE Computer Society.

12. I. A. Hiskens. Stability of limit cycles in hybrid systems. In *In: Proc. of the 34th Hawaii International Conf. on System Sciences*, pages 163–328, 2001.
13. W. Kühn. Zonotope dynamics in numerical quality control. *Mathematical Visualization*, pages 125–134, 1998.
14. D. Liberzon and A. S. Morse. Basic problems in stability and design of switched systems. *IEEE Control Systems Magazine*, 19:59–70, 1999.
15. J. Lygeros, C. Tomlin, and S. Sastry. Controllers for reachability specifications for hybrid systems. *Automatica*, 35(3):349–370, 1999.
16. R. Majumdar and M. Zamani. Approximately bisimilar symbolic models for digital control systems. In P. Madhusudan and S. A. Seshia, editors, *CAV*, volume 7358 of *Lecture Notes in Computer Science*, pages 362–377. Springer, 2012.
17. Ocaml Team. OCaml Web page. http://caml.inria.fr/ocaml/index.fr.html, 2013.
18. PPL Team. PPL Web page. http://bugseng.com/products/ppl/, 2013.
19. P. J. Ramadge and W. M. Wonham. The control of discrete event systems. *Proceedings of the IEEE*, 77(1):81–98, Jan. 1989.
20. G. Reißig. Computation of discrete abstractions of arbitrary memory span for nonlinear sampled systems. In R. Majumdar and P. Tabuada, editors, *HSCC*, volume 5469 of *Lecture Notes in Computer Science*, pages 306–320. Springer, 2009.
21. M. Senesky, G. Eirea, and T.-J. Koo. Hybrid modelling and control of power electronics. In *HSCC*, volume 2623 of *Lecture Notes in Computer Science*, pages 450–465, 2003.

Appendix 1: Sufficient Condition of Decomposition

Given a zone R, an invariant decomposition does not always exist. We give hereafter some geometrical conditions on the position of R that guarantee the decomposability of R when all the modes of the system are contractive, in the sense of Definition 1: For each $u \in U$, there exists $0 < \beta_u < 1$ such that, for all $x, y \in \mathbb{R}^n$:

$$\|\mathbf{x}(\tau, x, u) - \mathbf{x}(\tau, y, u)\| \leq \beta_u \|x - y\|.$$

For the sake of simplicity, we suppose that the switched system has only $|U| = 2$ modes, and the state space dimension is $n = 2$, but the reasoning extends to larger values of $|U|$ and n. We assume that matrix A_u associated with mode u ($u = 1, 2$) is invertible. Let $e_u = -A_u^{-1} B_u$ be the unique attractive equilibrium point associated with mode u ($u = 1, 2$). Let us define the "pure" switching rule $\mathcal{S}_u$ ($u = 1, 2$) which applies repeatedly mode u to any point $x \in \mathbb{R}^2$. Let $\mathcal{C}_1$ (resp. $\mathcal{C}_2$) be the τ-sampled trajectory issued from e_1 (resp. e_2) under $\mathcal{S}_2$ (resp. $\mathcal{S}_1$) (i.e., $\mathcal{C}_1 = Post_2^*(e_1)$ and $\mathcal{C}_2 = Post_1^*(e_2)$). Since each mode is contractive, and e_u is the unique equilibrium point associated with mode u, any trajectory under control $\mathcal{S}_u$ converges to the equilibrium point e_u ($u = 1, 2$), whatever the starting point of $\mathbb{R}^2$. In particular, $\mathcal{C}_1$ ends to e_2 and $\mathcal{C}_2$ to e_1, as depicted in Figure 11 for the boost converter (see examples 1 and 2).

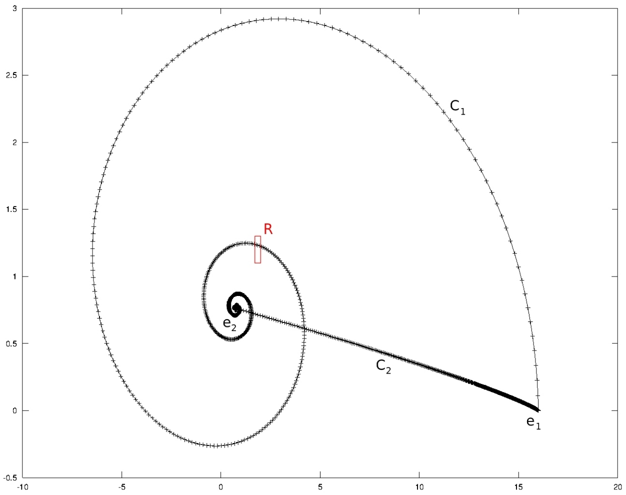

Fig. 11: Trajectories $\mathcal{C}_1$, and $\mathcal{C}_2$ and zone $R = [1.7, 2] \times [1.1, 1.2]$ for the DC-DC converter example

Theorem 4 *Let Σ be a sampled switched affine system as defined above. Suppose that the reference point O is in $\mathcal{C}_1 \cup \mathcal{C}_2$. If $R \subseteq \mathbb{R}^2$ is a box whose interior contains O, then there exists a positive integer k such that R is k-invariant.*

Proof Suppose $O \in \mathcal{C}_2$. (The case $O \in \mathcal{C}_1$ is symmetrical.) Consider a box R of interior $\mathring{R}$ with $O \in \mathring{R}$. There exists $\Delta_O > 0$ such that $\mathcal{B}(O, \Delta_O) \subseteq R$. Since $O \in \mathcal{C}_2$, we have:
(a) $e_2 \to^{\pi_1} O$, for some pattern $\pi_1 \in (1)^*$.
Furthermore, for all $x \in R$, we have:
(b) $x \to^{\pi_2} x_1$ for some $x_1 \in \mathcal{B}(e_2, \Delta_O)$ and some pattern $\pi_2 \in (2)^*$, because e_2 is an attractive equilibrium point;
(c) $x_1 \to^{\pi_1} x_2$ for some $x_2 \in \mathcal{B}(O, \Delta_O)$, because of (a) and because mode 1 is contractive. This is depicted in Figure 12. It follows from (b)-(c) that, for all $x \in R$: $x \to^{\pi_x} x_2$ for some $x_2 \in \mathcal{B}(O, \Delta_O)$ and some pattern $\pi_x \in (2^*1^*)$. Hence, we have: $\mathcal{B}(x_2, \Delta_x) \subseteq R$ for some $\Delta_x > 0$. Since, for any π_x, $Post_{\pi_x}$ is continuous, $Pre_{\pi_x}(\mathcal{B}(x_2, \Delta_x))$ [6] is an open subset of $\mathbb{R}^2$ containing x. Since R is a compact of $\mathbb{R}^2$, from the set $C = \{Pre_{\pi_x}(\mathcal{B}(Post_{\pi_x}(x), \Delta_x))\}_{x \in R}$, one can extract by Heine-Borel's theorem, a subset $C' = \{Pre_{\pi_{x_i}}(\mathcal{B}(Post_{\pi_{x_i}}(x_i), \Delta_{x_i}))\}_{i \in I}$, for some finite set of indices I, such that C' covers R and $\mathcal{B}(x_i, \Delta_{x_i})$ is R-invariant via π_i. This means that $C' \cap R$ is a k-invariant decomposition of R of the form $\{(V_i, \pi_i)\}_{i=1,\dots,m}$, where m is the cardinal of I, k the maximum length of $\pi_1, \dots, \pi_m$, and $V_i = \mathcal{B}(x_i, \Delta_{x_i}) \cap R$ is such that $\bigcup_{i=1}^m V_i = R$ and V_i is R-invariant via π_i $(1 \le i \le m)$. □

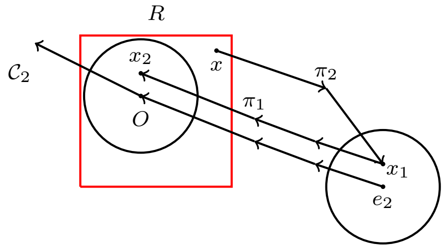

Fig. 12: Illustration of the proof

The theorem gives an interesting locality condition on O (location on one of the "pure" trajectories linking the equilibrium points), for ensuring the existence of k-invariant boxes R. This justifies *a posteriori* the existence of a decomposition for the zone R of the DC-DC converter example 2 since it overlaps trajectory $\mathcal{C}_1$. Note also that R can be arbitrarily small as far as it intersects $\mathcal{C}_1$ (or $\mathcal{C}_2$).

[6] For $\pi = u_1 \cdots u_m$, the operator Pre_π is defined by: $Pre_\pi(X) = \{x' \mid x' \to_\tau^{u_1} \cdots \to_\tau^{u_m} x \text{ for some } x \in X\}$.

Appendix 2: Case Studies

We now apply the decomposition procedure (enhanced for safety properties) for several examples. For each example, we will generate a k-invariant decomposition Δ of R satisfying $Unf_{\Delta}(R) \subseteq S$, thus proving that $Unf_{\Delta}(R)$ is a controlled invariant, and that the system is safe.

Example 4 Let us come back to the boost DC-DC converter of example 1. For R, we now take the box $[1.75, 1.95] \times [1.14, 1.26]$,[7] which corresponds to a medium value 1.85 for i_l with ± 0.1 for variability, and medium value 1.20 for v_c with ± 0.06 for variability. For the safety region, we take $S = [1.7, 2.0] \times [1.10, 1.30]$, which corresponds to an additional variability of ± 0.05 for i_l and ± 0.04 for v_c.

The application of the algorithm Decomposition to R and S, with $k = 10$ and $d = 4$ succeeds, yielding a k-invariant decomposition Δ of the form $\{(V_j, \pi_j)\}_{j=1,\dots,16}$ of R [8] satisfying $Unf_{\Delta}(R) \subseteq S$. The k-invariant decomposition Δ of R is depicted in Figure 13. The Δ-unfolding of R is depicted in Figure 14. It is divided into regions of two different colors corresponding to the different control modes: blue (resp. red) indicates that mode 1 (resp. 2) should be applied. The safety zone $S = [1.7, 2.0] \times [1.10, 1.30]$ is delimited in green.

The controlled system has been implemented using Octave [1]. The unfolded Δ-trajectory of the system starting at point $(1.75, 1.26)$, is depicted in Figure 15.

Other applications of the decomposition procedure are described in Section 5.

Example 5 (**Helicopter motion** [7]) The problem is to control a quadrotor helicopter to some position on top of a stationary ground vehicle, while satisfying constraint on the relative velocity. By controlling the pitch and roll angles, one can modify the speed and the position of the helicopter. Let g be the gravitational constant, x (resp. y) the position according to x-axis (resp. y-axis), $\dot{x}$ (resp. $\dot{y}$) the velocity according to x-axis (resp. y-axis), ϕ the pitch command, ψ the roll command. The possible commands for the pitch and the roll are: $\phi, \psi \in \{-10, 0, 10\}$. Since each mode corresponds to a pair (ϕ, ψ), there are 9 modes. The dynamics are given by the equation:

$$\dot{X} = \begin{pmatrix} 0\,1\,0\,0 \\ 0\,0\,0\,0 \\ 0\,0\,0\,1 \\ 0\,0\,0\,0 \end{pmatrix} \cdot X + \begin{pmatrix} 0 \\ g.sin(-\phi) \\ 0 \\ g.sin(\psi) \end{pmatrix}$$

[7] Note that we consider here a box R, which is smaller than the original box $R = [1.55, 2.15] \times [1.0, 1.4]$ used in example 3. This is because, the safety zone $S = [1.7, 2.0] \times [1.10, 1.30]$ considered here is itself included into the original R.

[8] The associated patterns are: $\pi_1 = (1122122122)$, $\pi_2 = (12121222)$, $\pi_3 = (12122122)$, $\pi_4 = (122)$, $\pi_5 = (2)$, $\pi_6 = (12)$, $\pi_7 = (12)$, $\pi_8 = (1)$, $\pi_9 = (1)$, $\pi_{10} = (1)$, $\pi_{11} = (12)$, $\pi_{12} = (12)$, $\pi_{13} = (2)$, $\pi_{14} = (2)$, $\pi_{15} = (12)$, $\pi_{16} = (221)$.

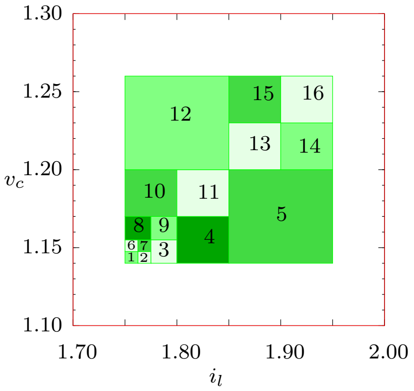

Fig. 13: Decomposition for boost converter for $R = [1.75, 1.95] \times [1.14, 1.26]$

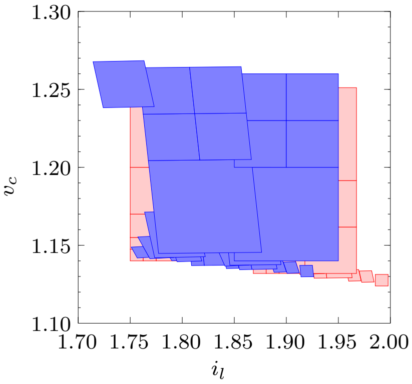

Fig. 14: Δ-unfolding for $R = [1.75, 1.95[\times[1.14, 1.26]$ where light red (resp. dark blue) indicates mode 1 (resp. 2), S corresponds to plot area

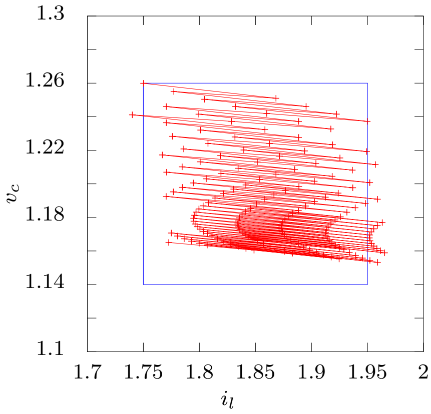

Fig. 15: Unfolded Δ-trajectory of the boost converter in plane (i_l, v_c), starting at $(1.75, 1.26)$ (R in blue, S corresponds to plot area)

where X is $(x, \dot{x}, y, \dot{y})^T$. The sampling period is $\tau = 0.1$. The variables x and y are decoupled in the equations and follow the same equations, so we focus on the control for x. We take $R = [-0.3, 0.3]\times[-0.5, 0.5]$ (i.e., $R = \{(x_1, x_2) \mid x_1 \in [-0.3, 0.3], x_2 \in [-0.5, 0.5]\}$). This corresponds to an equilibrium zone centered at the state $(0, 0)$ of the ground vehicle, and a variability of ±0.3 for position and ±0.5 for velocity. We take $S = [-0.4, 0.4]\times[-0.7, 0.7]$ for the safety region, which corresponds to an additional variability of ±0.1 for position and velocity. As for R, we take a box guessed manually from the equilibrium zone appearing in the numerical experiments and simulations of [7]. We take the same safety zone S as the one specified in [7].

The application of algorithm Decomposition to R and S with $k = 6$ and $d = 4$ succeeds, yielding a k-invariant decomposition Δ of R of the form $\{(V_i, \pi_i)\}_{i=1,\dots,10}$[9] satisfying $Unf_{\Delta}(R) \subseteq S$. The decomposition Δ is represented in Figure 16. The unfolding of R is depicted in Figure 17. The unfolding is divided into regions of three different colors corresponding to the different control modes: color red (resp. blue, green) indicates that mode 10 (resp. -10, 0) should be applied. The safety zone $S = [-0.4, 0.4] \times [-0.6, 0.6]$ in delimited in green.

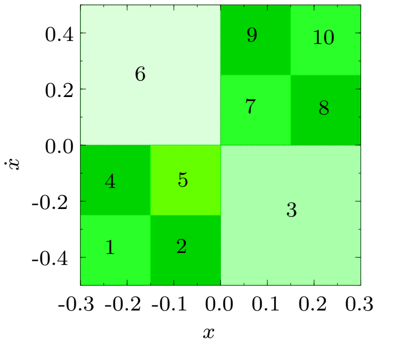

Fig. 16: k-invariant decomposition for helicopter motion

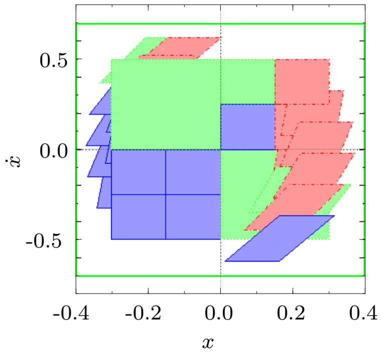

Fig. 17: Δ-unfolding for helicopter motion where blue (resp. red, green) indicates mode 10 (resp. -10, 0). (box S delimited in green)

The controlled system has been simulated using Octave. Figure 18 gives a simulation of the system represented in plane $(x, \dot{x})$, starting at point $(-0.3, 0.5)$.

Example 6 (**Two-room building heating** [9]) This is a simple heating model of a two-room building. Let $T = (T_1, T_2)^T$ be the state variable, where T_i is the temperature of room i ($i = 1, 2$). The dynamics are given by the equation: $\dot{T} = \begin{pmatrix} -\alpha_{21} - \alpha_{e1} - \alpha_f p & \alpha_{21} \\ \alpha_{12} & -\alpha_{12} - \alpha_{e2} \end{pmatrix} \cdot T + \begin{pmatrix} \alpha_{e1} T_e + \alpha_f T_f p \\ \alpha_{e2} T_e \end{pmatrix}$, where p is a mode of value 0 or 1, and the heat transfer coefficients and external temperatures are given by the values: $\alpha_{12} = 5.10^{-2}$, $\alpha_{21} = 5.10^{-2}$, $\alpha_{e1} = 5.10^{-3}$, $\alpha_{e2} = 3.3.10^{-3}$, $\alpha_f = 8.3.10^{-3}$, $T_e = 10$, $T_f = 50$. The sampling period is $\tau = 5$. We take $R = [20.25, 21.75] \times [20.25, 21.75]$. This corresponds to an equilibrium zone centered at state $(21, 21)$ with a variability of ± 0.75. For the safety zone, we take $S = [20, 22] \times [20, 22]$, as in [9].

[9] The associated patterns are: $\pi_1 = (-10 \cdot -10 \cdot -10 \cdot -10 \cdot -10 \cdot 0 \cdot 10)$, $\pi_2 = (-10)$, $\pi_3 = (0)$, $\pi_4 = (-10 \cdot -10 \cdot -10 \cdot 10)$, $\pi_5 = (-10)$, $\pi_6 = (0)$, $\pi_7 = (-10)$, $\pi_8 = (10 \cdot 10 \cdot 0 \cdot 0)$, $\pi_9 = (0)$, $\pi_{10} = (10 \cdot 10 \cdot 10 \cdot 10 \cdot 0 \cdot 10 \cdot -10)$.

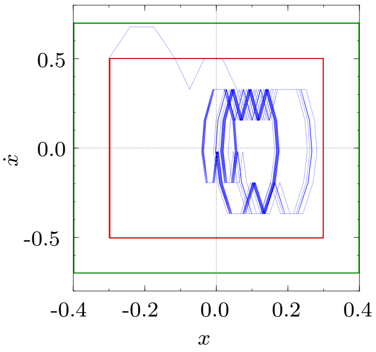

Fig. 18: Unfolded $\varDelta$-trajectory of helicopter motion in plane $(x, \dot{x})$ starting at $(-0.3, 0.5)$ (R in red, S in green).

The application of the algorithm Decomposition to R and S with $k = 4$ and $d = 2$ succeeds, yielding a k-invariant decomposition[10] $\varDelta$ of the form $\{(V_j, \pi_j)\}_{j=1,\dots,10}$ of R satisfying $Unf_{\varDelta}(R) \subseteq S$. The decomposition $\varDelta$ is depicted in Figure 19. The unfolding of R is represented on Figure 20. The unfolding is divided into regions of two colors corresponding to the different control modes: the red (resp. blue) color indicates that control 0 (resp. 1) should be applied. The safety zone S in delimited green.

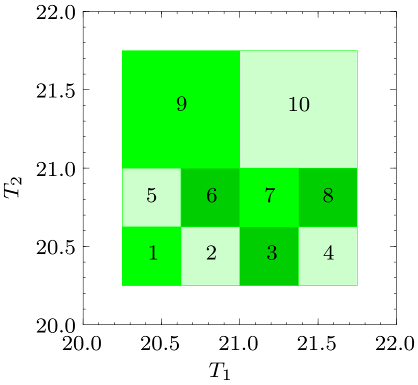

Fig. 19: k-invariant decomposition for heating system

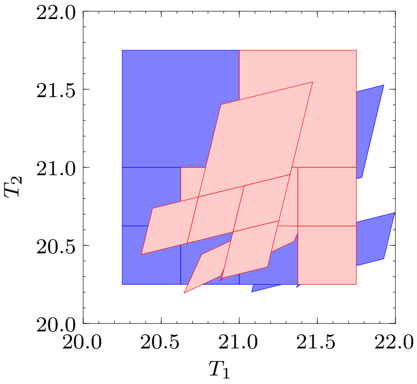

Fig. 20: $\varDelta$-unfolding for heating system where light red (resp. dark blue) indicates mode 0 (resp. 1). (S corresponds to plot area)

[10] The associated patterns are: $\pi_1 = (1010)$, $\pi_2 = (1)$, $\pi_3 = (10)$, $\pi_4 = (0)$, $\pi_5 = (0)$, $\pi_6 = (1)$, $\pi_7 = (0)$, $\pi_8 = (0)$, $\pi_9 = (0)$, $\pi_{10} = (10)$.

The controlled system has been simulated using Octave [1]. A simulation is depicted in Figure 21 for starting temperature point $(20.25, 21.75)$.

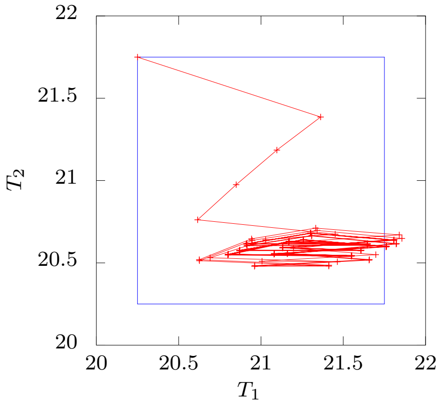

Fig. 21: Unfolded Δ-trajectory of heating system in plane (T_1, T_2), starting at $(20.25, 21.75)$ (R in blue, S corresponds to plot area)

Example 7 **Multilevel converter.** Using the decomposition procedure, we have synthesized a control for a case study originating from power electronics industry of high dimension ($n = 7$), satisfying a safety constraint. The control has been implemented and successfully physically experimented with a prototype. See [8].

Appendix 3: Control with disturbances

Zonotopes are useful for representing and manipulating efficiently convex polytopes. They allow us to extend easily the decomposition procedure in order to allow for small perturbations of the system dynamics (see, e.g., [13]). Using zonotopes, it is possible to introduce uncertainty or disturbance in our model. All the dynamics of the system are now of the form $\dot{x} = A_u x + B_u + \varepsilon$ where ε represents disturbance under the form of a n-dimensional vector belonging to a given box Ω of fixed size. We will use $\mathbf{x}(t, x, u, \varepsilon)$ to denote the point reached by the system at time t under mode u and disturbance ε from the initial condition x. This defines a transition relation $\rightarrow_{\tau}^{u,\varepsilon}$ given by:

$x \rightarrow_{\tau}^{u,\varepsilon} x'$ iff $\mathbf{x}(\tau, x, u, \varepsilon) = x'$ for x, x' in $\mathbb{R}^n$ and ε in Ω

We define $Post_u(X, \Omega) = \{x' \mid \exists \varepsilon \in \Omega,\ x \rightarrow_{\tau}^{u,\varepsilon} x'\}$. This definition naturally extends to $Post_\pi$ where π is a pattern. In order to handle disturbance, one replaces test $Post_\pi(W) \subseteq R$ of algorithm Find_Pattern by $\square(Post_\pi(W, \Omega)) \subseteq R$, where '$\square$' is the operator mapping a zonotope into the smallest enclosing box.

Example 8 (**Boost converter**) We consider the dynamics of the boost DC-DC converter (see examples 1 and 2) in presence of disturbances belonging to $\Omega = \{0\} \times [\frac{-0.064}{x_l}, \frac{0.064}{x_l}]$. These disturbances correspond to noise on the input voltage. They represent represent up to 8% of the value of the input voltage. With such disturbances, we have not found a control preserving the safety zone S defined in example 2, and we have taken a larger (i.e., more tolerant) safety zone defined by $S' = [1.65, 2.05] \times [1.10, 1.30]$. The decomposition procedure then succeeds for $k = 13$ and a $d = 5$: it generates a k-invariant decomposition Δ' of R satisfying $Unf_{\Delta'}(R) \subseteq S'$. The decomposition[11] Δ' is depicted in Figure 22. A simulation of the system starting at $(1.75, 1.26)$ is depicted in Figure 23.

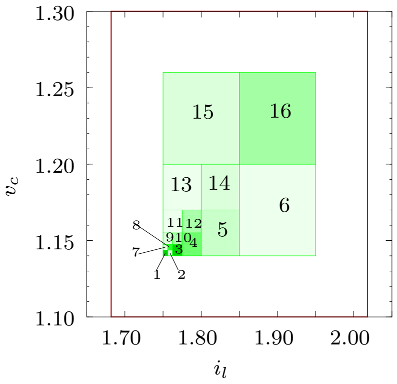

Fig. 22: k-invariant decomposition for boost converter with disturbances

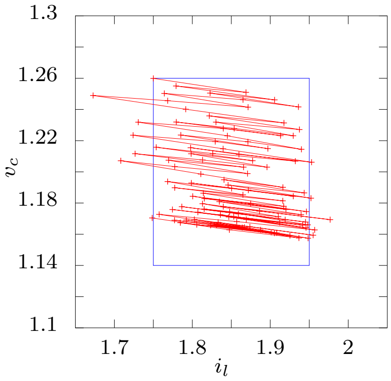

Fig. 23: Unfolded Δ-trajectory of the boost converter with disturbances in plane (i_l, v_c), starting at $(1.75, 1.26)$ ($R =$ in blue, S corresponds to plot area)

Example 9 (**Helicopter motion**) As done in [7], we will now solve the control problem with bounded disturbances to take into account a potential real-life environment. We use the same safe zone S as in example 5 and add the following possible disturbances $\varepsilon \in [-0.02, 0.02] \times [-0.1, 0.1]$. The decomposition procedure succeeds, and generates a new k-invariant decomposition Δ' with $Unf_{\Delta'}(R) \subseteq S$. The decomposition Δ' is depicted in Figure 24. A simulation of a run starting at point $(-0.3, 0.5)$ is presented in Figure 25.

[11] The corresponding patterns are: $\pi_1 = (1122121222)$, $\pi_2 = (1122122121222)$, $\pi_3 = (21121222)$, $\pi_4 = (12121222)$, $\pi_5 = (122)$, $\pi_6 = (2)$, $\pi_7 = (12)$, $\pi_8 = (12)$, $\pi_9 = (12)$, $\pi_{10} = (12)$, $\pi_{11} = (1)$, $\pi_{12} = (1)$, $\pi_{13} = (1)$, $\pi_{14} = (12)$, $\pi_{15} = (12)$, $\pi_{16} = (21221)$.

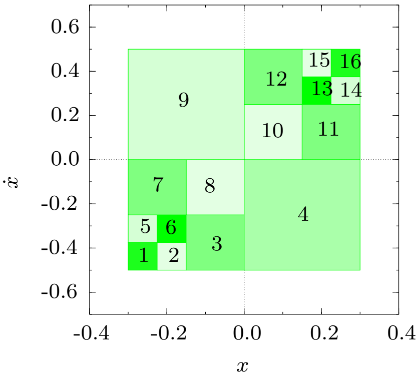

Fig. 24: k-invariant decomposition for helicopter motion with disturbances

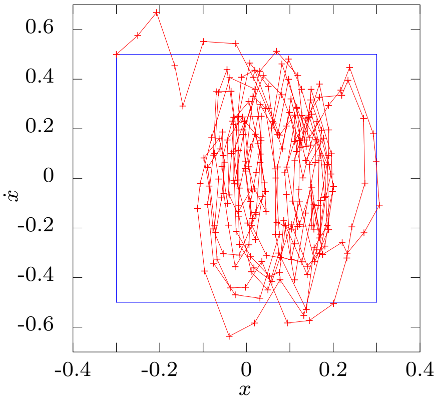

Fig. 25: Unfolded Δ-trajectory of helicopter motion with disturbances in plane $(x, \dot{x})$, starting at $(-0.3, 0.5)$ (R in blue, S corresponds to plot area)

Appendix 4: Example with $|R^{\infty}_{\Delta}| = \infty$

For this example, we use modes associated to repulsive homothetic transformation. There are 4 modes such that, close to each corner of the global box $R = [-1, 1] \times [-1, 1]$, there exists a fixed point for one of the mode. We take for the dynamics of the modes: $A_1 = A_2 = A_3 = A_4 = \begin{pmatrix} 1.5 & 0 \\ 0 & 1.5 \end{pmatrix}$, $B_1 = \begin{pmatrix} 0.6 \\ 0.6 \end{pmatrix}$, $B_2 = \begin{pmatrix} -0.6 \\ 0.6 \end{pmatrix}$, $B_3 = \begin{pmatrix} -0.6 \\ -0.6 \end{pmatrix}$, and $B_4 = \begin{pmatrix} 0.6 \\ -0.6 \end{pmatrix}$. The Δ-decomposition is presented in Figure 26. We have $V_1 = [-1, 0] \times [-1, 0]$ associated to pattern $\pi_1 = (1)$, $V_2 = [0, 1] \times [-1, 0]$ associated to pattern $\pi_2 = (2)$, $V_3 = [0, 1] \times [0, 1]$ associated to pattern $\pi_3 = (3)$, and $V_4 = [-1, 0] \times [0, 1]$ associated to pattern $\pi_4 = (4)$. A Δ-trajectory is depicted in Figure 27. One can see that the system appears to be chaotic and will not converge to a limit cycle.

Appendix 5: Visualizations of the Iteration of $Post_{\Delta}$

In Figure 28, we give the iterated images $Post^k_{\Delta}(R)$ of the boost converter benchmark for $k = 0, 10, 20, 40, 80, 100$. We see that for $k = 100$, $Post^k_{\Delta}(R)$ is completely located inside V_1. The controlled system converges to a single limit point.

Figure 29 shows the iterated images $Post^k_{\Delta}(R)$ of the two tanks benchmark for $k = 0, 5, 10, 15, 20, 25$. In the figures, it can be seens that starting with $k = 10$, the set $Post^k_{\Delta}(R)$ does not intersect the borders of the decomposition Δ. The system converges to a limit cycle (see also Figure 10 on page 16).

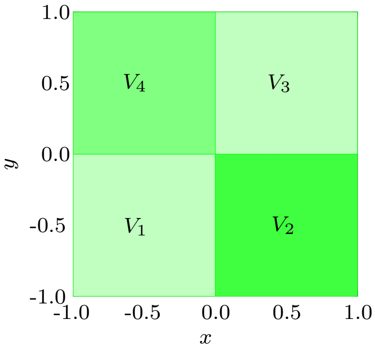

Fig. 26: Decomposition Δ of R for the non contractive example

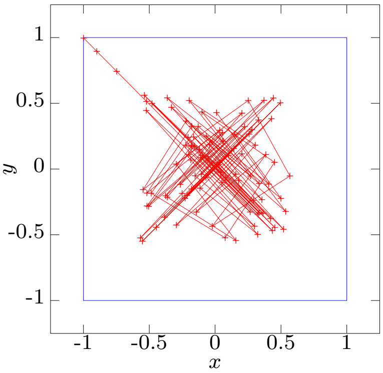

Fig. 27: Δ-trajectory for the non contractive example

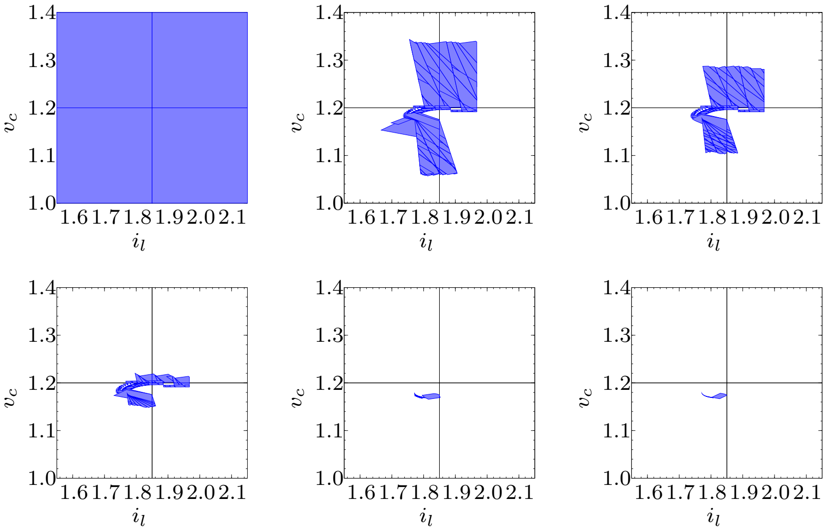

Fig. 28: Visualization of $Post_{\Delta}^{k}(R)$ of the boost DC/DC converter benchmark for $k = 0, 10, 20, 40, 80, 100$

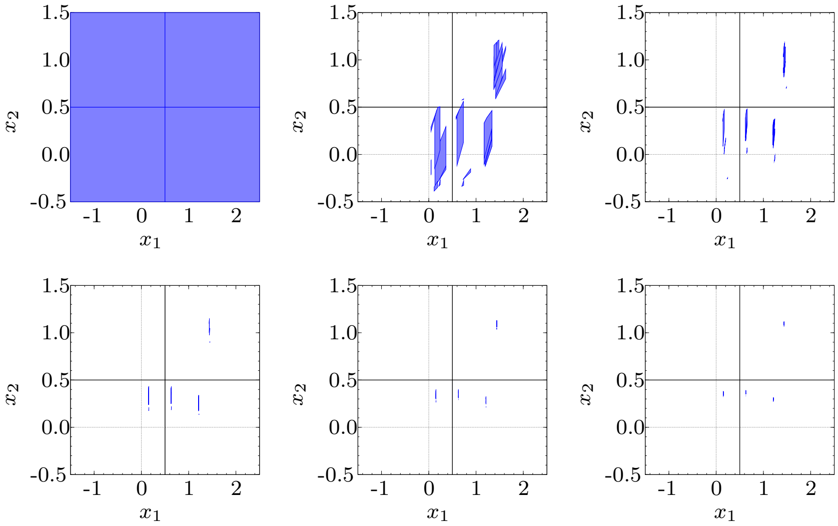

Fig. 29: Visualization of $Post_{\Delta}^{k}$ of the two tanks benchmark for $k = 0, 5, 10, 15, 20, 25$